iScience

CellPress
OPEN ACCESS

Article

Optimization of green ammonia distribution systems for intercontinental energy transport

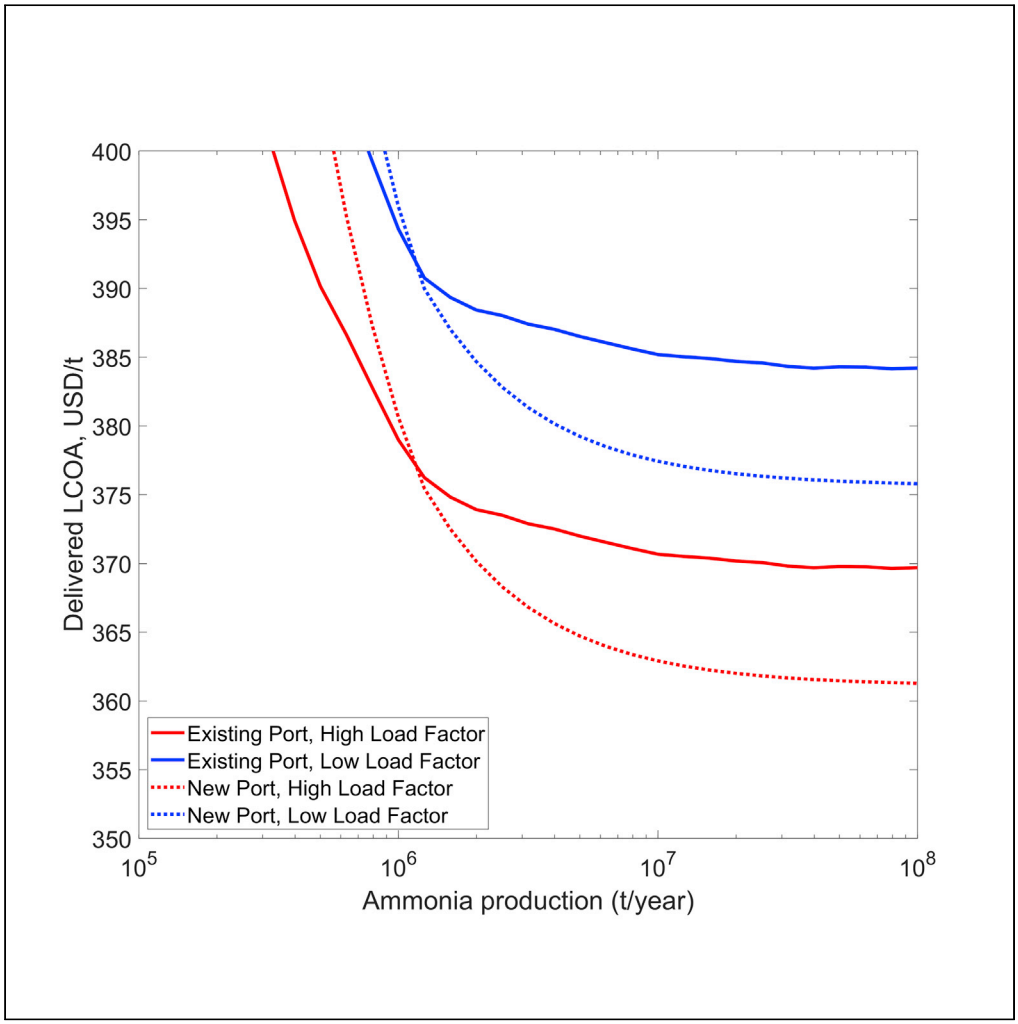

Nicholas Salmon, René Bañares-Alcántara, Richard Nayak-Luke

rene.banares@eng.ox.ac.uk

Highlights

An optimization model to represent a future green ammonia (NH_3) market is developed

Each supply chain element is described, including the relationship of cost to scale

NH_3 markets will tend toward a many-to-few trading pattern, unlike crude oil today

Limitations on available land may constrain production in optimal sites

Salmon et al., iScience *24*, 102903
August 20, 2021
https://doi.org/10.1016/j.isci.2021.102903

iScience

CellPress
OPEN ACCESS

Article

Optimization of green ammonia distribution systems for intercontinental energy transport

Nicholas Salmon,[1] René Bañares-Alcántara,[1,2,*] and Richard Nayak-Luke[1]

SUMMARY

Green ammonia is a promising hydrogen derivative which enables intercontinental transport of dispatchable renewable energy. This research describes the development of a model which optimizes a global green ammonia network, considering the costs of production, storage, and transport. In generating the model, we show economies of scale for green ammonia production are small beyond 1 million tonnes per annum (MMTPA), although benefits accrue up to a production rate of 10 MMTPA if a production facility is serviced by a new port or requires a long pipeline. The model demonstrates that optimal sites for ammonia production require not only an excellent renewable resource but also ample land from which energy can be harvested. Land limitations constrain project size in otherwise optimal locations and force production to more expensive sites. Comparison of current crude oil markets to future ammonia markets reveals a trend away from global supply hubs and toward demand centers serviced by regional production.

INTRODUCTION

Although the production potential for renewable energy far exceeds demand on a global level, many regions will suffer from energy deficit as they move to completely decarbonize by 2050 (Moriarty and Honnery, 2012; Babarit et al., 2018). Unless corrected, renewable deficits will either create energy poverty or retard global efforts to eliminate carbon emissions. Green ammonia, a derivative of green hydrogen, is a promising solution for these regions. It can be produced renewably, releases no carbon at point of consumption, and, compared to other hydrogen carriers, it is an energy dense liquid under mild conditions, meaning it can be stored cheaply on a timescale of months to years (Hank et al., 2020; Schmidt et al., 2019). It is already traded widely on international markets as a fertilizer (Lim et al., 2020). As an energy vector, it can be dispatched on demand – either as ammonia or having been cracked back into hydrogen. In either case, it can be combusted or used in a fuel cell (Valera-Medina et al., 2018). These properties enable ammonia to perform critical functions in decarbonized energy systems: it can carry hydrogen for fuel cell vehicles or for industry; it can provide grid peaking services when renewables or batteries cannot meet demand (Cesaro et al., 2021); it can balance energy seasonally; and it is the cheapest mooted option for a carbon-free shipping fuel (Van Hoecke et al., 2021).

The vast consumption of green ammonia invited by these applications, and the potential for energy shortages in some regions, will require a sophisticated system of global ammonia transport comparable in scale to the oil and gas sector today (Salmon and Bañares-Alcántara, 2021). Some authors have provided qualitative assessments of Power to X as an energy transport vector (Schmidt et al., 2019), and some have provided quantitative assessments which estimate the cost of energy transport between two points (Hank et al., 2020; Fúnez Guerra et al., 2020), or which consider the cost of energy transport as a function of shipping distance (Fasihi et al., 2021). However, to the best of the authors' knowledge, no study has yet considered the multilateral nature of power to energy trade using a quantitative approach. One unexplored area of particular significance is the trade-off between production and transport costs, as very good locations for water electrolysis are often located in isolated regions (Austria Energy, 2021).

This paper explains the development of a model which optimizes the global distribution of ammonia in a range of production and consumption scenarios. It is a high-level model intended to understand broad global patterns of ammonia production and transport, how ammonia markets will differ from current oil and gas markets, and how those markets may develop over time. The purpose of the model is not to

[1]Department of Engineering Science, University of Oxford, Parks Road, Oxford OX1 3PJ, UK

[2]Lead contact

*Correspondence: rene.banares@eng.ox.ac.uk

https://doi.org/10.1016/j.isci.2021.102903

precisely predict the distribution of ammonia in the long term or the exact locations at which ammonia will be produced; instead, it aims to demonstrate the major considerations which inform the selection of sites at which ammonia facilities should be located to minimize the cost of delivered energy. It gives an indication of the conditions required for local markets to grow, and the critical constraints on ammonia production that will affect future markets.

This work focusses on green ammonia (for the purposes of this work, green ammonia is produced by water electrolysis using renewable electricity, followed by a carbon-neutral ammonia synthesis step – in this case, an electrical Haber-Bosch loop, which is the only widely commercialized ammonia synthesis process with a technological readiness level which can make it deployable in the near term) only: by 2050, this approach is likely to be the cheapest way to make ammonia (even without carbon pricing), and it is the only option which is entirely carbon neutral (Nayak-Luke and Bañares-Alcántara, 2020; Osman et al., 2020; Salmon and Bañares-Alcántara, 2021).

Methodology

This section describes the formulation of a mixed integer linear program (MILP) to estimate the optimal set of ammonia producers given a specified demand at a range of global locations. The model optimizes the net present value (NPV) of delivered ammonia. It includes the costs at three nodes (production location, port, and destination), and transport between those nodes. Distribution within the destination country is not included (further discussion of the possible impact of local distribution is provided in demand constraint section). Where production sites are coastal, the model can bypass land transport from production location to existing port; instead, the model will construct a new port at those production sites if it is more cost effective to do so. A full description of the model is found in the STAR Methods section.

There are three sets of nodes in the model: exporters (S_{Ex}), importers (S_{Im}) and ports (S_{Po}). The total NPV for a set of nodes NPV_{Si} is calculated according to

$$NPV_{S_i} = \sum_{i \in S_i} CAPEX_i + G_{EY} \sum_{i \in S_i} OPEX_i \qquad \text{(Equation 1)}$$

Equation (1) can be extended to the NPV for transfer between nodes, $NPV_{Si,Sj}$, using the relevant CAPEX and OPEX values for the transfer cost. The parameter G_{EY} relates the annual OPEX to the NPV and can be interpreted as the plant lifetime at a discount rate of zero which results in an NPV equivalent to that calculated using the actual plant lifetime at the nominated discount rate. It is calculated according to

$$G_{EY} = \frac{(1+G_i)^{G_y} - 1}{G_i(1+G_i)^{G_y}} \qquad \text{(Equation 2)}$$

where G_I is the discount rate and G_y is the plant lifetime. This model uses a discount rate of 7% and a project lifetime of 20 years, which results in a value of G_{EY} equal to 10.59 years. Estimating project lifetimes for much of the equipment required in green ammonia plants is challenging, as the robustness of this relatively new technology is not yet fully understood; however, the model is not strongly sensitive to this result, and increasing the plant lifetime by 50% only increases the parameter G_{EY} by 17%.

Based on the above, the delivered levelised cost of ammonia (DLCOA) can be calculated from the sum of the NPVs for each set of nodes and node transfers, all divided by the net present annual flow (calculated as the equivalent years times the sum of all flows from exporters to ports):

$$DLCOA = \frac{NPV_{S_{Ex}} + NPV_{S_{Po}} + NPV_{S_{Im}} + NPV_{S_{Ex},S_{Po}} + NPV_{S_{Po},S_{Im}}}{G_{EY} \sum_{Ex \in S_{Ex} Po \in S_{Po}} F_{Ex,Po}} \qquad \text{(Equation 3)}$$

Using this approach, the DLCOA does not depend on the year of construction. While the NPV for a plant with a fixed CAPEX and OPEX will be lesser if it is constructed in the future, the value of the net present annual flow is discounted at the same rate; the effects of this change to the numerator and denominator cancel out. The DLCOA is therefore used as the objective function and for comparison between different sites, since it is not impacted by the year of construction.

This model considers demand profiles for 2030, 2040, and 2050. An optimum solution is calculated for each year independently. However, there are no sites which produce ammonia in 2040 or 2050 that are not also active in earlier years, although the recipient of ammonia from a specific site may change. Therefore,

although the demand profile in 2050 is calculated at a certain point in time, it is reflective of a supply network that has grown over more than two decades.

Linearization

An entirely rigorous global optimization of an ammonia market is well beyond the capacity of modern simulation technology. In order to reduce the problem to a manageable complexity, a large number of variables were preoptimized, and simplified into linear formats.

The most significant of these variables is the levelised cost of ammonia production (PLCOA). Note the distinction between the production and delivered levelised costs of ammonia (PLCOA and DLCOA, respectively) – the latter includes transport and storage costs, whereas the former only includes the costs at the supplier. Nayak-Luke and Bañares-Alcántara (Nayak-Luke and Bañares-Alcántara, 2020) rigorously optimized the islanded production cost of green ammonia at over 500 locations based on historical hourly wind and solar profiles (including the costs of electricity, electrolysers, hydrogen storage, backup power, air separation, ammonia synthesis, and water desalination). In each of the ten regions they considered around the globe, they identified ten optimal sites (only nine sites were identified in Southeast Asia, meaning a total of 99 sites are used here). At the time of writing, this represented the most comprehensive global review of the cost of green ammonia production at different locations.

The ammonia locations available to the model correspond to these optimal sites, with the PLCOAs calculated by Nayak-Luke and Bañares-Alcántara for a multinational corporation in 2030 used as the cost of ammonia production at those sites. Because the production cost of ammonia is by far the largest contributor to the delivered cost of ammonia, excluding nonoptimal production sites has limited impact on model output but greatly reduces its complexity. In addition, the PLCOA at 13 further sites was modeled using the same approach and input data as Nayak-Luke and Bañares-Alcántara; these include sites considered promising by other authors (Armijo and Philibert, 2020) or which are the proposed location of large hydrogen/ammonia facilities. The relevant data for those locations are shown in Table 1.

Like oil and gas markets, the market for ammonia demand is expected to be seasonal. Importers will require ammonia either when domestic primary energy production is low (because of a lack of sun and wind) or when local energy consumption is high (because of seasonal energy demands). Additionally, the supply of ammonia will vary seasonally, matching local meteorological conditions at the production site. The ammonia costs used in this model partially account for this seasonal variation in production by oversizing some equipment and incorporating hydrogen storage. This enables the ammonia plant to operate year-round, albeit at reduced rates during periods of low renewable energy availability.

To "smooth out" this annual variation, additional buffer capacity may be required. The costs of such a buffer are not included in this model but are unlikely to significantly impact the model solution, as the storage of ammonia, even over large timescales, is cheap compared to its production (Cesaro et al., 2021) (as discussed in sensitivity results section, six months of storage would increase DLCOA by around 17 USD/t, or 5%). This represents the maximum increase in costs which could occur if seasonal differences in production were factored into the model. This higher cost would only be required if the prospective supply and demand locations had highly mismatched profiles. Additionally, the locations selected as optimal rarely have extended periods of reduced production; typically they have low PLCOAs because they have high overall process utilization. Therefore simplifying production and demand into annual average rates is unlikely to substantially impact total costs or the overall distribution of a global ammonia market.

The largest costs of green ammonia production come from the renewable energy generators (wind turbines and solar panels) and hydrogen electrolyzer units. Although some of the equipment in renewable energy generators and electrolysis units benefit from increased project scale (e.g. hydrogen purification equipment), both of these components are mostly modular and their costs therefore scale linearly. Accordingly, Zauner et al. (Zauner et al., 2019) found that electrolysers cease to benefit from economies of scale at a project size of ~100 MW (for reference, operating a 100-MW electrolyzer at 100% load factor would produce ~ 17,000 tpa of hydrogen, which can be used to produce slightly less than 10^5 tpa ammonia).

However, the balance of plant, in particular, the Haber-Bosch (HB) loop for ammonia synthesis, and the air separation unit (ASU) are conventional chemical engineering units and have a scale exponent between 0.6

Table 1. Additional locations which are considered likely production sites of green ammonia

Location	Country	Latitude	Longitude	PLCOA (USD/t)	Rated wind fraction (%)	Full load hour equivalent per year	HB load factor	Electrolyzer rated power (MW)	NH3 synthesis (MW)
Patagonia (Argentina) (Armijo and Philibert, 2020)	Argentina	−44.5	−71	383	53	2850	67	930	67
Callide (CSIRO, 2020)	Australia	−24.5	150.5	375	20	2375	78	2,310	79
Eighty Mile Beach (Asian Renewable Energy Hub, 2020)	Australia	−20	120.5	551	12	1580	67	2,010	77
Port of Pecem (Bellini, 2021)	Brazil	−3.5	−39	329	0	2442	46	2,150	121
Calama Valley (Armijo and Philibert, 2020)	Chile	−22	−69	378	7	1684	63	2,450	90
Patagonia (Chile) (Armijo and Philibert, 2020)	Chile	−52.5	−71	298	84	4845	72	1,160	84
Taltal (Armijo and Philibert, 2020)	Chile	−25	−70	309	23	2370	76	2,220	80
Eqianqi (Keating, 2020)	China	41	109	352	0	2442	47	1,890	107
Ain Beni Mathar (Ennassiri et al., 2019)	Morocco	34	−2	350	0	2106	47	1,730	99
Boujdour (Ennassiri et al., 2019)	Morocco	26	−14	289	27	2788	79	1,500	67
Laayoune (Ennassiri et al., 2019)	Morocco	27	−13	273	41	3349	78	1,580	76
Ouarzazate (Ennassiri et al., 2019)	Morocco	31	−7	350	11	1946	69	1,920	78
Tarfaya (Ennassiri et al., 2019)	Morocco	28	−12.5	291	35	2935	75	1,620	76

Electrolyzer and ammonia power demands are shown for a plant size with an average energy supply of 1 GW. Citations provide details surrounding the existing proposals for the use of those sites.

and 0.8 (Sanchez and Martín, 2018; Hochman et al., 2020; Fernandez and Hatzell, 2020). The largest single-train ammonia plants in the world have a capacity of ~ 1 million tonnes per annum (MMTPA) (Vasquez and Hapes, 2019); after this point, multiple trains need to be constructed, and the benefits of economies of scale are expected to fall. Figure 1B shows the impact of scale on ammonia synthesis costs (excluding hydrogen production), based on a scale factor of 0.7 up to a maximum capacity of 1 MMTPA; above this production rate, modeling green ammonia production costs as linear introduces minimal error. Two cases are shown: one for a high load factor renewable energy supply in which the ammonia plant only represents 16% of production NPV and a second case for a lower load factor supply in which the ammonia plant represents 25% of production NPV. For the locations considered in this model, which encompass a wide range of renewable energy profiles, 90% have an ammonia synthesis cost which falls between 16% and 25% of the total production cost.

Pipelines are used to transport ammonia from production sites to local ports; although trucking ammonia is also possible, pipelines are far more cost effective for all distances at large scales (Yang and Ogden, 2007). The difference between land procurement and labor costs between countries, which may affect pipeline costs, is neglected here for simplicity. A full description of the pipeline cost estimation is provided in the STAR Methods section, and results are shown for a 100-km pipeline in Figure 1C. It shows pipeline costs are nonlinear with respect to flow rate up to a scale of ~ 10 MMTPA ammonia; at larger flow rates, increasing pipeline size has a smaller proportional effect on the total pipeline CAPEX. At flow rates $>10^6$ tonnes per annum of ammonia, the price of ammonia pipeline transport falls to around 1% of the approximate delivered cost of ammonia, which is between 350 and 450 USD/t for the locations considered. Therefore, even though it is not strictly linear, the error introduced by the linearization of pipeline costs is small in comparison to the total delivered cost, although the error will grow in proportion to the length of the pipeline. The cost/t/km of ammonia pipeline was taken from the linear regression of the rigorously estimated costs between 1 and 10 MMTPA.

Ammonia storage is required at both the local and the destination port. At large scales, it is most cost-effective to store ammonia in insulated tanks at −33°C and atmospheric pressure, storage at atmospheric temperature under pressure requires far more steel to withstand the static pressure of the fluid, and is thus more

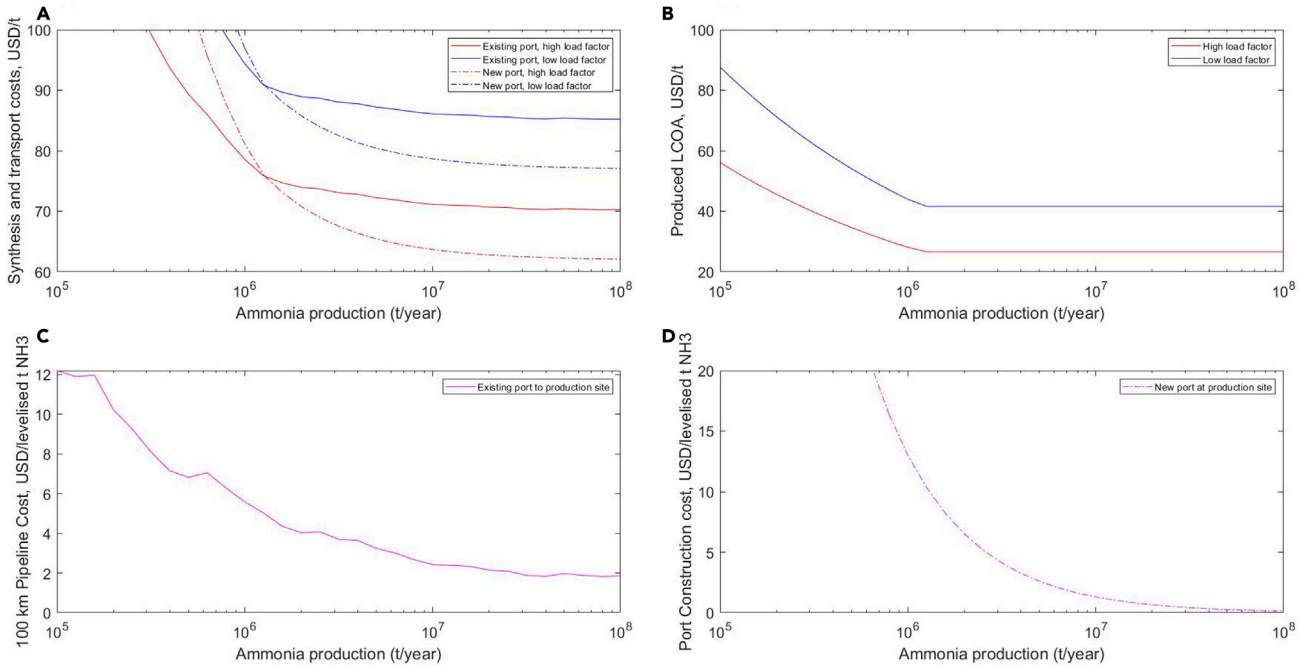

Figure 1. Impacts of scale on various components of green ammonia production and transport, excluding hydrogen production

(A) Synthesis and transport costs.

(B) Synthesis costs only.

(C) Pipeline costs (100 km).

(D) New port costs

costly (even though no refrigeration unit is required to recondense any boil off). The CAPEX of these tanks is reported in Leighty and Holbrook (Leighty and Holbrook, 2012) and confirmed by Bartels (Bartels, 2008). The cost of recondensing boiled-off ammonia is estimated assuming a boil-off rate of 0.05%/day (Al-Breiki and Bicer, 2020), a coefficient of performance (COP) for the refrigeration unit of 2, an average tank level of 50%, and an electricity price of 80 USD/MWh at the port. Storage volumes forecast by the model are comparable to existing very large ammonia tanks (~ 60,000 t) (Leighty and Holbrook, 2012); around this scale, increasing storage requires the production of additional tanks. Consequently price reductions per tonne will not be observable as production rates increase, and linearizing storage costs will not introduce error.

The model also enables the construction of new ports adjacent to some ammonia production sites, if those sites are coastal. The cost of a regular container port can be in the order of ten billion USD (Economic Research Institute for ASEAN and East Asia, 2018); often very large costs 1 billion USD can accrue for dredging alone (Songhurst, 2014). However, the complex facilities that are required at container ports, or even onshore liquefied natural gas (LNG) terminals, are not necessary for ammonia export locations. Many of the sites identified by Nayak-Luke and Bañares-Alcántara (Nayak-Luke and Bañares-Alcántara, 2020) are in isolated locations without existing ports, and the sole purpose of a new port would be transfer of ammonia from shore to ship. One design which achieves this simple function cheaply is a single mooring point (SMP), which is essentially an anchoring point for a ship, connected to ammonia tanks onshore via a short subsea pipeline. Although these SMPs cannot provide full maintenance and service to ships as would be available for a regular port, they do not require significant additional onshore infrastructure or dredging and are already in use for liquid propane gas (LPG) (Raaijmakers, 2012). Their cost is approximately 100 million USD (Moffatt and Nichol, 2005). There are no land transport costs associated with constructing a new port, and it is assumed that ships which berth there do not accrue a berthing fee. The impacts of port construction on the ammonia cost are shown in Figure 1D; although DLCOA falls rapidly with scale, the impact on the project NPV (the objective function) is linear with respect to the binary decision variable to include a port.

The overall impacts of scale using a rigorous cost approach (i.e. without linearization) are shown in Figure 1A. It includes a land transport distance of 100 km and an ocean transport distance of 5,000 km (using

Table 2. Ship sizes used in the model

Ship Name	DWT	Draft (m)	LOA (m)	Charter cost (USD/hired day)	Berthing fee (USD/berthing day)	Fuel use (t NH_3/ocean day)
Small Handysize	11,568	9	132	31,071	32,500	29
Large Handysize	27,834	10	177	44,455	63,132	40
Handymax	54,049	12	227	66,025	112,500	52
Panamax	82,618	12	288	97,096	150,000	75

Deadweight tonnage (DWT), draft and overall length (LOA) are average sizes from the AIS database.

the largest ship size shown in Table 2). The synthesis and transport costs shown on the y axis include all costs associated with ammonia production and transport except the hydrogen production costs; they therefore represent the sum of all costs which may be affected by project scale. For the cases in which an existing port is used, the costs become a weak function of production around a plant size of 1 MMTPA, at which point the Haber–Bosch process ceases to benefit from economies of scale. For that reason, the model will be constrained to production capacities 1 MMTPA to limit linearization errors. For cases in which a new port is constructed, economies of scale continue to benefit production up until around 10 MMTPA, after which the impact of new port costs become small.

Ocean transport costs

The cost of ocean transport includes several components: the chartering of the ship, port berthing costs, the ship fuel, and fees for using either the Suez or Panama canals. These components convert linearly into a shipping cost for ammonia based on the total number of trips required each year. Costs were estimated for a ship making a return journey; while cost reductions are sometimes possible if the shipping route has synergies with other commodities, this is unlikely for liquefied gas tankers.

The ships used for transporting ammonia are expected to be comparable to those used for liquid propane gas (LPG), which has a similar boiling point to ammonia of −42°C (National Institute for Standards and Technology, 2020), although LNG ships can also be used for ammonia transport. Data extracted from the global Automatic Identification System (AIS) indicate there are presently over 2,500 ships capable of transporting LPG or LNG, the precise characteristics and nomenclature of which vary between ship builders. For the purposes of this model, they are grouped into four categories as summarized in Table 2. The largest of these ships (Panamax) is typically used only for LNG (not LPG) at present, but it is reasonable to assume that a global ammonia economy would make use of this size to minimize costs. The larger ships considered here will be fully refrigerated, although the smallest size considered (small handy size) may be more economically constructed using a semirefrigerated, semipressurized design (Wärtsilä, 2021).

For calculating the shipping cost, the model uses the largest ship which is able to dock at the supplier port, as constrained by both the ship's draft and LOA (overall length) relative to the size of the port. Data were obtained for existing ports from ShipNext (ShipNext, 2021). It was assumed that ships of all sizes could dock at ports which had been newly constructed (because single mooring points are built away from the shoreline, they typically do not impose draft or LOA restrictions on docking ships).

Chartering of ships is the most common method for international transport of liquid fuels. It is not common for energy exporters to own their own ships; doing so carries substantial capital risk and requires maritime expertize which energy producers may not possess. Chartering also enables more flexibility of production schedules. The chartering rates of maritime vessels are highly volatile; in 2020, for instance, LNG charters for 160,000 m^3 ships ranged from between 20,000 and 120,000 USD/day (Homan and Klass, 2020). To some extent, this volatility was caused by the coronavirus disease 2019 pandemic, but it is also typical for the industry, in which changing ship availability and seasonal energy needs cause significant price fluctuations. Charter costs are estimated using the method described in Rogers (Rogers, 2018) and capital costs reported by the ERIA (Economic Research Institute for ASEAN and East Asia, 2018), which also provides estimates of berthing costs. An additional 2% was added to the chartering costs for brokerage fees, and a further 2,600 USD/day were added for insurance.

It is assumed that the ships considered burn ammonia for fuel in a two stroke engine. For simplicity, the cost of this fuel is given as the cheapest ammonia available at the supplying port (estimated by the sum of the

production cost and pipeline costs). The fuel use for ammonia ships is estimated by Ash and Scarbrough (Ash and Scarbrough, 2019) whose estimates are based on slow steaming (around 18 nautical miles/h); this slow rate tends to be more economical when fuel costs are high, which they are expected to be using renewable fuels. The total ammonia transported by a ship is given by the usable capacity of the ship minus the fuel used in transport. The usable capacity of the ship is 94% of its total capacity; this accounts for a filling limit of 98% at the supply port to prevent overpressure of the vessel, and a heel remaining in the vessel at the demand port of 4%.

Shipping distances are estimated using a tool provided by S&P Global (Platts, 2021); the cost per trip was estimated both for routes with and without interoceanic canals and the cheaper option selected. Fees for the Suez and Panama canals, like ship chartering fees, are highly variable. Rogers (Rogers, 2018) reports the return trip cost through the Panama Canal in USD/MMBtu of LNG, which was used to estimate the overall canal fee for a liquefied gas tanker of a nominated volume. It was assumed the cost in the Suez Canal is equal to that in the Panama Canal. In general, because the price of ammonia as shipping fuel is high, it is preferable for ships to pay the canal fee and reduce the journey distance, but in some circumstances where the difference in distance is small, it may be preferable to detour around the canal.

Local production in countries which also have a demand for imported ammonia is allowed, but that ammonia must be delivered to an existing port in that country (either by pipeline or by ship from a port on the coastline).

Constraints

There are three major constraints in the model, which originate from material balances at the supplier, port and consumer.

$$Cap_{Ex} \geq \sum_{Po \in S_{Po}} F_{Ex,Po} \quad \forall\ Ex \in S_{Ex} \qquad \text{(Equation 4)}$$

$$Cap_{Im} \leq \sum_{Po \in S_{Po}} F_{Po,Im} \quad \forall\ Im \in S_{Im} \qquad \text{(Equation 5)}$$

$$\sum_{Ex \in S_{Ex}} F_{Ex,Po} = \sum_{Im \in S_{Im}} F_{Po,Im} \quad \forall\ Po \in S_{Po} \qquad \text{(Equation 6)}$$

Equation (4) requires that each exporting node cannot export more than its capacity; Equation (5) requires that each importing node at least satisfies its ammonia demand. Note that delivery to any port within the destination country can contribute toward satisfying the demand constraint. Equation (6) requires that ports be neither producers nor consumers of ammonia; they must export as much as they import.

Supply constraint. The maximum supply, C_{Ex}, is set by the lesser of the global maximum site capacity and the local maximum site capacity. The renewable energy generation capacity of the recently announced Asian Renewable Energy Hub (Asian Renewable Energy Hub, 2020) is 100 TWh; of the 26 GW of generation capacity, 23 GW will be dedicated to green ammonia production (generating $\sim$ 88 TWh of energy); assuming an LHV conversion efficiency to hydrogen of 70%, 6.6% of hydrogen LHV used for compression, and 3% of LHV for synthesis to ammonia (as per Nayak-Luke and Bañares-Alcántara [Nayak-Luke and Bañares-Alcántara, 2020]), the ammonia production from this plant will be approximately 9.5 MMTPA, which is significantly larger than any existing (conventional or green) ammonia facilities. Assuming that other locations are able to achieve a comparable scale, the global maximum site capacity was set at 10 MMTPA.

The local maximum project capacity was estimated for each supplier location based on land availability. Using a land consumption of 5.5 km^2/installed GW for solar (Kakoulaki et al., 2021), and 200 km^2/installed GW for wind (Ruiz et al., 2019), the project area per MMTPA capacity was calculated. The area of the remaining plant equipment required was considered negligible.

The local maximum site capacity is constrained by the total land area and by the available land area. Firstly, no single project could consume more than 3% of the total land area of a location, which typically limited capacity on small islands which otherwise had suitable renewable profiles for ammonia production. Three percent is a suitable factor as recommended by Kakoulaki et al. (Kakoulaki et al., 2021) to avoid competition with other uses for the land. Secondly, no site could consume more than 3% of the available land with capacity for either wind or solar generation in the target country. Data to estimate available land was

Table 3. Demand scenarios used as constraints in the MILP model

Location	Use	2030 demand (MMTPA)	2050 demand (MMTPA)
Algeciras (Spain)	Shipping	0.39	13
Antwerp (Belgium)	Shipping	0.39	13
Fujairah (UAE)	Shipping	1.17	39
Germany	Domestic energy	1.65	55
Hong Kong	Shipping	0.81	27
Japan	Domestic energy	3	100
Los angeles (USA)	Shipping	0.59	20
Panama canal	Shipping	0.59	20
Rotterdam (Netherlands)	Shipping	0.39	13
Shanghai (China)	Shipping	0.81	27
Singapore	Shipping	0.81	27
South Korea	Domestic energy	2.52	87
	Shipping	0.81	27

obtained from the Food and Agriculture Organization of the United Nations (Food and Agriculture Organisation of the UN, 2021).

Available area for solar panels was taken as the sum of barren land, shrubland, and urban areas (as rooftop solar); at present, it is assumed that marine solar panels are not practical. Wind turbines compete less for land than solar panels (because land with wind turbines on it can be used for other purposes), meaning they are allowed on grasslands and herbaceous croplands which may also be used for farming. If a production location is coastal, offshore turbines are also allowed within 12 nautical miles of the shore (Ruiz et al., 2019). However, wind farms are not allowed in urban areas and typically must have a setback distance of between 0.5 and 2 km from settlements. This impact of this limitation on land available for wind turbines is highly variable on local restrictions and national urbanization. An European Union (EU) study found that, of available land for wind turbines, the amount which met setback requirements varied from as low as 1% (in Luxembourg) to as high as nearly 50% (in Greece); the average rate was 15%, which was used as a general limit in this model in absence of more rigorous studies globally (Ruiz et al., 2019).

Of the 112 sites considered in the model, 77 were unconstrained by land availability and could produce ammonia at the global maximum rate, 17 were constrained by the total land availability (all of them islands), 5 were constrained by land available for solar, and 13 were constrained by land available for wind.

Demand constraint. Implementing the demand constraint described in Equation (5) requires predictions of future demand; these are summarized in Table 3. Because energy systems which use ammonia as a reserve fuel will require both strategic and financial support from government, we assume that only countries with specific intentions to import chemical energy will have local demand in the future. It is assumed here that all imported chemical energy is in the form of green ammonia; equivalences between green ammonia and hydrogen are calculated on an higher heating value (HHV) basis. Three major economies have publicly announced energy import strategies: Japan (100 MMTPA ammonia imports by 2050) (Japanese Ministry of Economy, Trade and Industry, 2021), Germany (340 TWh = 55 MMTPA ammonia imports by 2050) (Gerbert et al., 2018), and South Korea (16.9 MMTPA H_2 is equivalent to 105 MMTPA ammonia on an HHV basis by 2050). Since South Korea does not specify which fraction of its hydrogen will be locally produced, it is assumed that the breakdown will be the same as Germany's: 20% will be produced locally to maintain energy security while the balance will be imported.

The demand constraint considered in this model requires only that ammonia be delivered to any local port in the relevant country, rather than specifying a particular location within the country where the ammonia will be used. The costs of distribution may be a significant portion of the DLCOA and will depend on the use case. For grid stability or if it is to be cracked back into hydrogen, ammonia will require a pipeline to an industrial center, the costs of which would be comparable to pipelines in supply countries (~1% of DLCOA). If ammonia is to be used for transport applications (e.g. fuel cell electric vehicles), then a more complicated

distribution network which may include road, rail, and small pipeline distribution may be required: the costs of transporting ammonia from a port to a central node of this distribution network would be small in comparison to the total cost of such a network. In either case, it is not likely that the distribution costs will significantly affect the production sites and maritime routes selected by this optimal model. The most significant impact of including distribution costs is that ammonia would need to be redirected to a port further away from its original point of origin; the largest such redirection possible in this model is 1040 km (From Hamburg to Rostock or vice versa), which would translate to an increase in the transport cost of 4 USD/t – in most cases, the redirection distance will be even smaller and therefore cheaper. Therefore, while the distribution costs may be substantial, the costs upstream in the supply chain required to optimize those distribution costs are comparatively small.

Shipping fuel will also generate plentiful demand for ammonia by 2050. The International Energy Agency (IEA) estimates that 1,400 TWh of renewable fuels will be required by 2050, equivalent to 225 MMTPA ammonia (Tattini and Teter, 2020). Although there are a large number ports worldwide which can supply bunker fuel, bunker capacity is highly concentrated in a small number of ports (Ban et al., 2015). Therefore, the top ten bunker ports in the world, listed in Table 3, are used as delivery sites in this model, since they will consume a significant majority of the bunker fuel. OPEC's World Oil Outlook (Jan et al., 2020) provides an estimate of the distribution of bunker fuel to major shipping hubs globally in 2045. This Organization of the Petroleum Exporting Countries (OPEC) estimation is used to calculate the fraction of the total 225 MMTPA ammonia demand supplied to major global shipping ports (assuming the fraction of the total global bunker fuel required at each port is unaffected by substituting the oil products modeled by OPEC with green ammonia). Unlike the case of energy-importing nations, the model requires that ammonia used for maritime fuel be delivered precisely to the port at which it will be consumed.

Although PLCOA data are provided for 2030, demand estimates suitable to 2050 are considered here; while the PLCOAs are likely to fall between 2030 and 2050, it is assumed for simplicity that they will fall at approximately even rates, meaning the best sites for producing ammonia in 2030 remain the best sites in 2050 (other possibilities are also considered in sensitivity results section). Demand in 2030 is estimated to be 3% of demand in 2050, consistent with Japan's ammonia strategy (Japanese Ministry of Economy, Trade and Industry, 2021). The model assumes exponential growth in the market occurs between the forecast demand in 2030 and 2050 to estimate the 2040 demand, which is reflective of the rapid growth in installed infrastructure that is expected to occur in the decades preceding 2050.

Design constraints. Several other constraints are required to ensure realistic results from the model. Pipeline transfers from supplier to port are only allowed within a single region; typically, regions reflect national borders, but they can be subnational (in the case of large offshore islands such as Hawaii and Tasmania) or multinational (in the case of Continental Europe and Southern Africa). If a supplier is to be active, it must produce more than 1 MMTPA ammonia, as discussed in linearization section. Storage size at both supply and demand ports must be adequate to provide suitable buffer between the upstream production plant and the downstream ships, which is achieved by two constraints:

$$V_{Po} \geq x_{Po} 1.5 P_{VMax_{Po}} \quad \forall Po \in S_{Po} \qquad \text{(Equation 7)}$$

$$V_{Po} \geq \sum_{Ex} F_{Ex,Po} \Big/ 52 \quad \forall Po \in S_{Po} \qquad \text{(Equation 8)}$$

Equation 7 requires that, assuming the port is active ($x_{Po} = 1$), the storage volume must be more than 150% of the volume of the largest ship which is able to dock at that port (as specified by Yoo et al.) (Yoo et al., 2013). Equation 8 requires that the storage volume be more than a single week's worth of production; this constrains fewer tank designs than Equation 7 but is necessary to enable scheduling flexibility if ships are arriving with high frequency.

RESULTS AND DISCUSSION

Base case results

The results from the model for its base case are shown in Figure 2. For comparison, a representative map of current global crude oil flows is also provided. The crude oil market is dominated by three major supply regions, in particular by the Middle East, which supplies energy to a range of consumption regions. The trend for ammonia is reversed: a range of supply regions are forecast to provide two concentrated demand

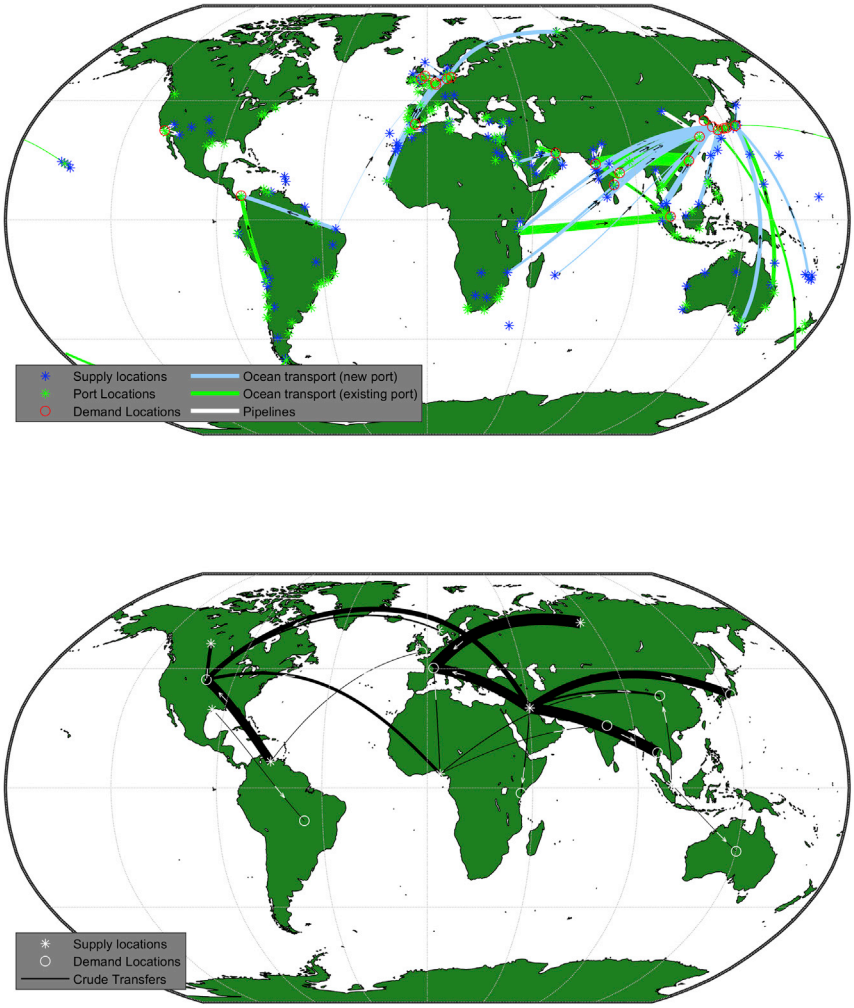

Figure 2. Energy flows in different markets

Top (A) Base case forecast for green ammonia transfer in 2050. Transfer of ammonia from supplier to destination is represented by great circle lines, but actual maritime distances were used in calculation. Thicker lines indicate larger ammonia flows. Bottom (B) Current global oil distribution, provided for comparison - adapted from Global Energy Assessment (Global Energy Assessment, 2012) and the Energy Information Administration (US Energy Information Administration, 2017). Flows on (B) represent major flows (>1 EJ/year) only, and cluster groups of nearby countries into regions for readability.

regions (East Asia and Europe). The pattern for crude indicates that, to a significant extent, the cost advantage of extracting oil in the Middle East justifies the cost of transport, even to demand centers very far from the supply port. Two factors lead to this result: the abundance of supply in the Middle East and the high energy density of crude oil, which leads to comparatively cheap transport costs.

On the supply side, the cost of ammonia transport only partially explains the differences in its distribution pattern compared to crude oil. The PLCOA for this data set varies from 273 to 551 USD/t between the cheapest and most expensive locations considered. Although this range is wide, it is distributed across the globe. In other words, while some locations for ammonia production are significantly preferable to others, these excellent locations are not concentrated in a specific region like the Middle East. Consequently, production is economically viable in many regions in cases with large global demand. Fasihi et al., who also considered green ammonia costs at different global locations, drew a similar conclusion, showing that cheap ammonia was available in all regions of the world, and was not concentrated in a specific location (Fasihi et al., 2021).

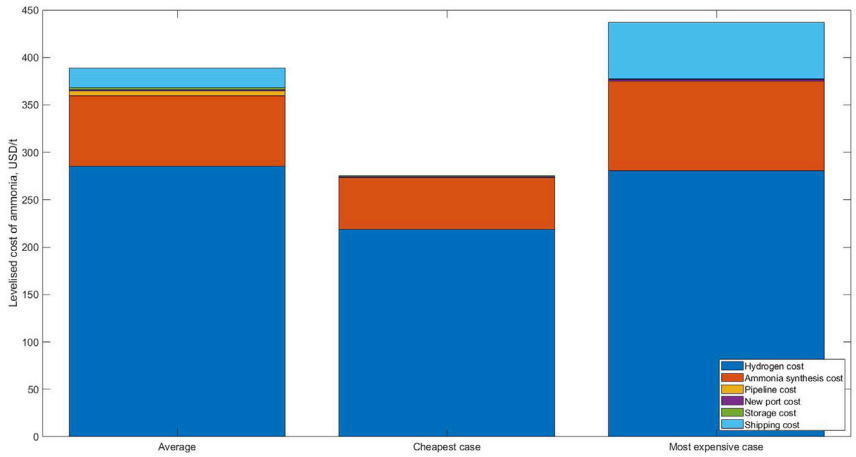

Figure 3. Breakdown of delivered cost of ammonia on average, and for the cheapest and most expensive cases
The most expensive case represents the marginal cost of ammonia in the model.

The contribution of transport to the DLCOA is much less than the range observed in ammonia production costs. On average, the total contribution of ammonia transport to the DLCOA is 20 USD/t or about 5% of the average DLCOA, as shown in Figure 3. The largest transport cost observed was 79 USD/t or 18% of the DLCOA for that route (Hawaii to Japan). Even in this case, the unusually high transport cost originates from the small size of the local port, which forces the use of a small Handysize ship at much greater costs per ton than a Panamax.

Typically, therefore, a large difference in transport cost is required to differentiate two sites with (comparatively) small proportional differences in PLCOA. For instance, the cheapest site at which ammonia can be produced, Laayoune in Morocco (PLCOA = 273 USD/t) also supplies the cheapest delivered ammonia to Germany (about 3,750 km away), beating out several more expensive production sites that are closer to Germany, including some in Europe itself. However, Cape Grim (PLCOA = 310 USD/t) supplies cheaper ammonia to Japan than Laayoune; because the distance between Laayoune and Japan is so large (about 20,000 km, via a canal), cheaper ammonia comes from a closer region.

Although Cape Grim is the cheapest supplier of ammonia to Japan in this model, there are a number of more proximate locations to Japan whose DLCOA could be more competitive, but which are too small to house a green ammonia plant. In particular, a number of islands near Japan in the Pacific have excellent profiles for ammonia; Kwajalein in the Marshall Islands, for instance, has a PLCOA of 324 USD/t. The constraints on its land area, however, afford it an annual production capacity of just 4,500 tpa. Similarly, Sonnblick in Austria could supply green ammonia at a very competitive rate (its PLCOA is 318 USD/t), but its annual production capacity is only 55,000 tpa; building a pipeline to Germany would not be justifiable at those flowrates.

Since the DLCOA is only a weak function of the transport distance, ammonia production will tend to occur in locations with the best resource, as per the crude oil distribution graph. However, where the capacity of the main production region for crude oil is comparable in size to the total global demand, the capacity of individual sites in this ammonia model is much less than total global demand. Total global demand in the base case for 2050 is 464 MMTPA ammonia, and individual sites are limited to 10 MMTPA ammonia; many are smaller due the additional constraints imposed by land restrictions. In the short term, where demand is relatively small, individual production sites may be able to supply many demand sites; as demand grows, additional sites will need to come online, and most production sites will increasingly supply only a single demand location. Video S1 is an animation that shows the transition of the fuel supply from few-to-many to many-to-few.

While it is possible that ammonia sites by 2050 will exceed 10 MMTPA of production, it is unlikely they will exceed it by an order of magnitude (the current largest single-site ammonia plant in the world has a capacity of slightly more than 4 MMTPA [Taillon, 2016]) Of the sites in this model which had the capacity to supply

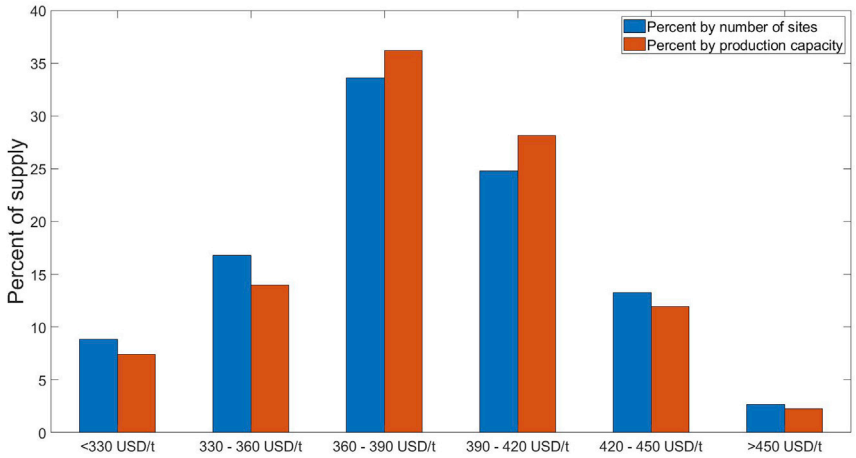

Figure 4. Distribution of ammonia capacities by PLCOA, grouped by number of sites and by total production capacity

10 MMTPA, the average land area required was 950 km^2 (for reference, this is roughly equal in area to 13,000 football fields or the area of the city of Dublin). As land limitations become more constraining toward 2050 due to competition from local renewable energy production, it is unlikely that it will be possible to construct megaplants which are significantly larger than 10 MMTPA.

Figure 4 illustrates the impact of land restrictions on the availability of low-cost ammonia. Although more than 25% of sites considered in this model can produce ammonia for less than 360 USD/t, only about 20% of ammonia can be produced at those sites. In other words, sites with excellent conditions for ammonia production (<360 USD/t) are more land constrained than sites with good conditions for ammonia production (>360 USD/t). One significant driver of this effect is that excellent conditions for ammonia production are often found on isolated islands, which have consistent wind profiles but do not have enough land to support a large ammonia facility.

The consequence of these land restrictions is that the capacity of excellent locations for ammonia production is exhausted quickly as demand rapidly grows toward the middle of the century; ammonia must therefore be sourced from more expensive locations. The impact of increasing demand on the delivered cost of ammonia is shown in Figure 5. At very small scales, when demand is concentrated in Japan, increasing the production rate of ammonia reduces the delivered cost per ton, because although all ammonia is produced very cheaply in Cape Grim, it requires a new port to be constructed which will have low utilization. As utilization of that new port improves with increasing production, the average DLCOA drops to a minimum between 10 and 20 MMTPA of total global demand (in the order of the largest plant size allowable in the model). After this point, two new factors emerge which begin to increase the average cost of ammonia. Firstly, demand begins to come online in a wider range of locations due to the requirements of the maritime industry, requiring new and more expensive supply sites to be used to avoid the very high transport costs from the best production sites. Secondly, supply capacity at the best production sites is exhausted, and more expensive sites must be identified; these are sometimes located further afield from demand sites. As a consequence of these two factors, DLCOA begins to increase rapidly with demand. By 2050, the marginal cost for delivering additional ammonia is 140 USD/t (around 6 USD/GJ) more than the lowest cost achievable – see Figure 3.

Although distance is only a weak factor in determining the delivered cost of ammonia, it can become more significant if there is a large land distance between the supply location and a port. The average pipeline cost in this model is small (5 USD/t); but the cost of transporting ammonia by pipeline is larger than the cost of transporting it by ship on a per kilometer basis. On average in this model, pipeline transport costs about 2 USD/t/100 km, whereas ocean transport averages 0.5 USD/t/100 km. Many of the good locations for ammonia in this model are coastal, meaning pipeline costs do not have a large impact on delivered costs. However, locations which are more than 1,000 km from their nearest port and are not coastal, face a competitive disadvantage approaching 20 USD/t ammonia; at this magnitude, other locations with

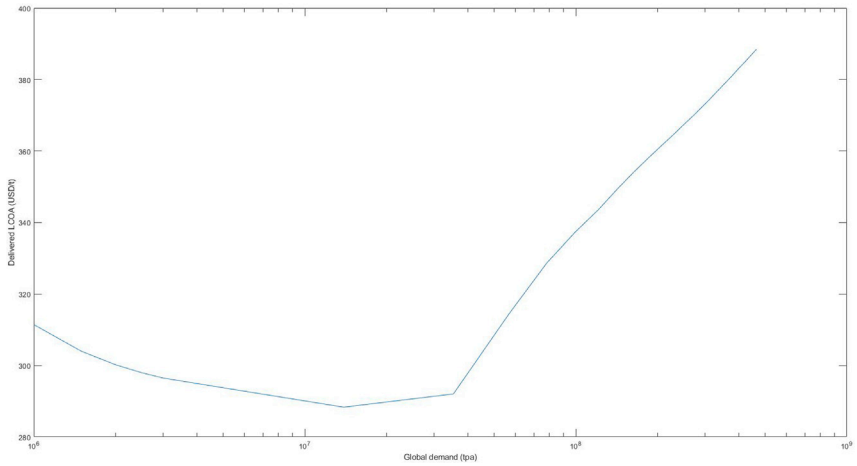

Figure 5. Optimum global average delivered cost of ammonia as a function of demand

The distribution of demand globally assumes Japan is the first to import green ammonia; after Japan has met its 2030 target, demand in all countries grows equally up to the 2050 demand specified in Table 3.

less favorable renewable profiles will begin to become active in order to avoid these transport costs. Additionally, water costs may be larger for noncoastal sites; while the PLCOA factors in water consumption costs assuming desalination is used, no water transport costs are assumed. For inland sites in areas of water stress, pipelines may need to be duplicated to enable two-way flow: water to the site and ammonia away from the site.

Because a number of green ammonia projects have already been announced, those locations were included in the dataset of prospective suppliers of green ammonia or hydrogen. In some cases, the PLCOAs from those locations were extremely competitive; for instance, 3 of the sites recommended for use in Morocco had a forecast PLCOA below 300 USD/t by 2030. Such low prices for green ammonia have not previously been reported; they can be achieved in Morocco because they have very high solar radiation and wind speeds and because the estimate is made using 2030 equipment costs and favorable financial conditions (a discount rate of 3.3% on most equipment). The presence of these excellent locations meaningfully adjusts the model's forecast, increasing the fraction of supply which originates in Chile, Morocco and China. This emphasizes the importance of identifying not only the optimal countries for ammonia production at a global level but also of identifying the specific locations within those countries at which ammonia can most cheaply be produced.

In other cases, those locations were noncompetitive and did not supply ammonia in the final model; Antofagasta in Chile, for instance, is due to commence hydrogen production in 2024 (Jones, 2020); however, its PLCOA is greater than 400 USD/t. When this is considered in tandem with the large distance between Chile and most of global demand, it is unlikely this site will be competitive. Similarly, the proposed location for the Asian Renewable Energy hub (listed as Eighty Mile Beach in Table 1) has a PLCOA greater than 500 USD/t, which is the worst of any location in our study. Although this is not promising for the forecast PLCOA in this region, there are two reasons the PLCOA estimate provided here may be overstated. Firstly, the model relies on reanalysis data of meteorological conditions; while this is largely accurate, it can differ from actual data in some locations. The low load factor for wind which is predicted in this location may indicate errors in reanalysis data. Secondly, the approach of Nayak-Luke and Bañares-Alcántara (Nayak-Luke and Bañares-Alcántara, 2020) adjusts the cost of installed renewable energy based on national data; in the case of Australia, they estimate these costs to be significantly higher than other regions. If the Asian Renewable Energy Hub is able to secure cheaper turbines and PV panels than predicted in the PLCOA model, it may be able to produce ammonia at a more competitive rate.

Because the capacity of a single ammonia site is likely to be much less than the demand in demand centers and the transport cost of ammonia is fairly low, supply sites will typically ship green ammonia to the closest demand center. This means long distance ammonia transport – such as the German government's proposal to import green hydrogen from Australia (Australian Department of Industry, 2020) – is unlikely to be efficient. The overall cost of green ammonia, and hence decarbonization, would be lower if Australia were only

to export its finite supplies of cheap green ammonia regionally. It is important that national interests do not trump the optimal global ammonia distribution, or the cost of decarbonization will increase for all.

This model forecasts only two major demand hubs for 2050 (East Asia and Europe), which contrasts with the current distribution of crude oil shown in Figure 2. This reflects current government policy but may also occur organically as green ammonia markets develop. Since demand-side management, electrification, batteries, and local energy storage (e.g. pumped hydro) may be cheaper than ammonia for short-term storage, and most countries have at least one site where ammonia can be produced locally at a cost competitive with the average cost forecast in this model, ammonia import is unlikely on a large scale unless a country's renewable energy potential is less than its energy demand. At present, this is only expected to be true for parts of East Asia and Europe. Fuel for the maritime industry is one exception to that general observation, since it must be bunkered in a small number of key ports and because ammonia's properties make it specifically well-suited to that duty.

Overall, patterns of ammonia distribution will tend to be far more regional than existing patterns of distribution which exist for crude oil. The availability of land in locations with good renewable energy profiles is a critical parameter for the provision of affordable green ammonia; land shortages encourage production in more expensive locations.

Sensitivity results

To understand the impact of various key parameters on the global distribution of ammonia, sensitivity analyses were run to understand their impact on the optimum ammonia distribution. The results are summarized in Table 4; Table 5 provides more detail on the infrastructure requirements estimated for the 2030, 2040, and 2050 cases.

New port CAPEX and berthing costs were included in the sensitivity analysis as there are limited data available for cost estimation; the sensitivity analysis shows that they have very little impact on the DLCOA or on the distribution of ammonia (since the number of ports and suppliers, and their average distance from demand centers, was largely unaffected by changes to these parameters).

Daily chartering costs for ammonia ships will vary over the lifetime of ammonia plants according to energy demand and ship supply, and the sensitivity analysis shows this will impact the DLCOA; however, it does not substantially affect which sites are optimal for ammonia production. Varying chartering fees by 50% only varies the average shipping distance for ammonia by ~5%. Varying charter costs therefore impacts the cost of fuel in demand countries but has limited impact on location selection for new green ammonia plants.

There is a relationship between the (time-varying) charter costs and ammonia storage, which may influence the times of year at which ammonia is transported. The average cost of ammonia storage in this model is 2.3 USD/t of ammonia; the average storage time is 3.4 weeks (i.e. 1.7 weeks storage at the supply port, and an additional 1.7 weeks storage in the demand port). In that context, it may be more cost-efficient to store ammonia locally at the supplier until the charter cost has fallen. Constructing six months of storage (three months at the supply port and three months at the demand port) would increase the ammonia price by ~17 USD/t; if this enabled transport to be performed when the chartering price was low, this storage may on net reduce the DLCOA. Similarly, it may be cheaper for importing nations to stockpile large quantities of ammonia when the charter price is low than to pay expensive shipping costs. This implies that there is a relationship between the size of storage and the time-dependency of the chartering cost and that the optimum storage size could be significantly larger than the sizes predicted in this model. The optimum size will also be influenced by the seasonal energy patterns in supply and demand locations, and the benefit of additional storage is magnified for larger transport distances.

Land availability and maximum plant capacity have a similar sized impact on the DLCOA to the charter cost, but a more significant impact on the location and number of facilities. Lessening these constraints enables more capacity to be extracted from the best locations; tightening the constraints requires more expensive, more distant locations to be used to satisfy demand. However, because the individual plant production capacity is much less than the total demand, the impact of these changes on the DLCOA is not as large as changing the total demand.

Table 4. Sensitivity results

Sensitivity	Units	Value in base case	Value in sensitivity case	Average DLCOA (USD/t)	DLCOA range	Active suppliers	Number of existing ports	Average transport distance (km)	Fraction of full-sized plants
Base	–		–	392	–	52	15	4,406	67%
New port CAPEX	million USD	100	50	392	0.5	52	15	4,441	67%
			150	392		52	17	4,406	67%
Berthing Fee[a]	thousand USD/day	150	75	391	1	52	16	4,444	67%
			225	392		52	14	4,389	67%
Charter Fee[a]	thousand USD/day	97	48.5	383	17	53	15	4,636	69%
			145.5	400		55	15	4,207	70%
Land availability	% available land	3	1.5	401	11	60	18	5,057	61%
			4.5	390		51	14	4,199	79%
Max. plant Capacity[b]	MMTPA	10	7.5	402	16	67	18	4,848	78%
			12.5	386		44	13	4,399	60%
2050 demand	MMTPA	464	242.5	371	39	25	5	3,886	52%
			727.5	410		78	20	5,346	71%
Year	Year	2050	2030	328	64[c]	3	1	5,725	33%
			2040	347		9	3	4,896	50%

[a]The base value and sensitivity values shown for berthing fee and charter fee pertain to the largest ship size (the Panamax); costs for smaller ship sizes were scaled in the same proportion (i.e. ±50%).

[b]The sensitivity range used for this case was ±25%, rather than ±50% because the model was not able to satisfy the demand constraints when the maximum plant capacity was reduced by 50%.

[c]The sensitivity range here refers to the difference between the cheapest case (2030) and the base case (2050).

Two modifications to the demand were included: one modification varied the total demand in 2050 and the other considered much smaller demands that will exist in the decades preceding 2050. These factors had by far the most significant impact on the DLCOA, largely because at very high demands, the problem is highly constrained. In the high-demand case for 2050, 90% of available supply is required to satisfy demand, which requires almost every site to be active. Under these conditions, there is likely to be competition for ammonia from the various demand centers. Knowing this, first-mover investors in coming decades will be incentivized to pursue fixed-price arrangements with suppliers in order to secure access to the finite supply of low-cost ammonia from the optimal sites. This market competition may risk the optimal distribution of ammonia from a limited number of production sites; while it will reduce prices for some actors, it will increase prices on average. The very high fraction of available supply which is required to satisfy demand demonstrates that, although a large number of sites with very high capacities were considered in this analysis, further sites need to be identified which can be used for affordable ammonia production. The additional sites listed in Table 1 indicate that many such sites exist but have yet to be reported upon in the literature. The identification of these further sites will impact the optimal solution, but the broad trend – that is, exceptional sites may supply ammonia over long distances, but in general production will be located close to consumption – is unlikely to change unless production capacity in newly located exceptional sites is so large it is able to meet a significant fraction of global demand.

In comparing the production for 2030, 2040, and 2050, improvements to the PLCOA from technology development were not included, as there is considerable uncertainty in the rates at which the various technologies required for green ammonia will improve. If the reductions in the PLCOA have an equal impact on all sites, then the resulting distribution of ammonia would be unchanged, although a faster-than-expected reduction in PLCOA may stimulate additional demand. However, it is likely that some sites will improve more rapidly than others; in particular, the price of solar and electrolyzer installation will fall more quickly than the price of wind (International Renewable Energy Agency, 2019). In the current model for ammonia production, the excellent locations with a PLCOA <330 USD/t in 2030 rely on very reliable wind supply, which means high utilization of equipment is possible. As the price of solar technology falls relative to wind, however, locations with high-intensity sunlight will catch up to wind installations. Similarly, as the price of electrolysers falls relative to wind, obtaining very-high-capacity factors will become less critical to the affordability of ammonia, an effect observed by

Table 5. Total global equipment demands and ammonia productions for the 2030, 2040, and 2050 cases

Global totals	2030	2040	2050
Installed solar capacity (GW)	12	21	2491
Installed wind capacity (GW)	21	87	242
Installed electrolyzer capacity (GW)	22	155	1223
Installed ammonia capacity (GW)	1.2	7.1	52
Ammonia production (MMTPA)	14	80	464

Nayak-Luke and Bañares-Alcántara (Nayak-Luke and Bañares-Alcántara, 2020) when comparing PLCOAs from 2019 to 2030. The precise impact of this technological improvement should be the subject of further investigation, but it is forecast that the impact of reduced solar and electrolyzer costs will skew the distribution shown in Figure 4 to the left. In other words, extremely low ammonia prices will not be restricted to sites with reliable wind, but will also be available to a much greater number of locations with excellent solar resources. If those sites are concentrated in regions with sufficient land availability (for example, India, the Middle East, and Northern Africa), those sites will become global hubs for ammonia production because transport costs are small compared to production costs. However, if those sites are evenly distributed globally (as good sites for ammonia production presently are), then ammonia trade will tend even more strongly toward the regional distribution displayed in Figure 2.

One further source of PLCOA reduction as demand increases are the economies of mass production associated with manufacturing individual components. Electrolysis units will benefit to the most significant extent from these economies of mass production, as the other high cost components (wind turbines and solar panels) are likely to have achieved high levels of industrial efficiency already from their use in the power industry. This potential cost reduction is not considered in this optimization problem and may counteract the increase in DLCOA caused by growing demand in this model. However, analysis on the economies of mass production of electrolysers from the National Renewable Energy Laboratories (Mayyas et al., 2019) suggests that economies of mass production will cease impacting costs at a production rate of ~ 50 GW/year. Beyond this point, electrolyzer costs are primarily a function of material demands. To meet the target demand by 2050, assuming all electrolysers required for ammonia production are constructed between 2025 and 2050, an annual production rate of 48 GW/year is required; since other hydrogen projects which do not use ammonia as a carrier will also be proceeding, it is likely that global production will substantially exceed 50 GW/year, and economies of mass production will no longer drive down project costs significantly.

One interesting result from the demand analysis by year is the average distance traveled by ammonia falls by almost 30% over time. At very low demands, only a small number of sites are active; these are uncommonly good locations for ammonia production and their large distance from demand centers is justified by the low production costs. As demand begins to increase, the good sites proximate to demand centers begin to become active, and the average transport distance falls. This confirms the hypothesis formed in base case results section: transport costs are small in comparison to the range of PLCOAs, so sites with extremely competitive ammonia production (the left-hand tail of Figure 4) are cost-competitive regardless of their location. In general, though, since no region produces ammonia much more cheaply than any other, ammonia production will tend to occur close to demand centers to minimize the transport distance.

Limitations of study

To some extent, the results from the model are limited by the finite list of available production sites. An important area for further research is the inclusion of a larger number of sites with suitable optimal production rates. The inclusion of additional sites may change the specific locations from which ammonia is imported; however, it is unlikely to change the broad global patterns described in this discussion.

If a large cluster of new sites with very low production costs is identified (in Morocco, for instance, which has an excellent solar resource), then it is possible that such a cluster of sites will become the dominant supplier of green ammonia for the globe, akin to the distribution of crude oil from the Middle East today. However, there are several reasons such a pattern is unlikely to emerge. Firstly, even though this paper reports several very low PLCOAs in multiple regions, the difference between those PLCOAs is not large enough to justify the increased shipping distance. It is not likely that there exist unrecognized sites with significantly lower PLCOAs than those identified here

that would justify a single location shipping to demand sites on the other side of the world. Secondly, the production capacity at that cluster of sites would need to be two orders of magnitude higher than the production capacity at any existing ammonia site in order to meaningfully adjust the fuel supply predicted here from a many-to-few pattern into a few-to-few pattern. The land requirements for such large production are not likely to be sustainable by a single country or region, particularly where that land is likely to be required for local energy generation for decarbonized electricity grids. Where a many-to-few pattern dominates fuel supply, it will always encourage a regional distribution of fuel. Thirdly, because of the hydrogen strategies of many supply countries (including at least Australia, Chile, Norway, Morocco, and Saudi Arabia (Salmon and Bañares-Alcántara, 2021)), it is likely that a wide number of suppliers will emerge around the world. Therefore, although data limitations mean it is not possible to predict the exact distribution of green ammonia, the sites used in this model can still provide valuable insight into the nature of future ammonia markets.

Conclusions

This optimization of a global ammonia market has shown that ammonia transport need not add a significant amount to its delivered cost, indicating it is a suitable vector for intercontinental energy transport. Nevertheless, the optimal distribution of green ammonia will occur on regional scales (~ 5,000 km), rather than ultralong distances (~ 20,000 km), which may render some very long-range bilateral agreements (e.g. between Germany and Australia) inefficient. Minimum costs for individual producers are obtained at scales of around 1 MMTPA, but production at good facilities will need to be much larger than 1 MMTPA to satisfy global demand efficiently.

If they have excellent renewable energy profiles, locations far from demand centers may be preferable to more local production sites, particularly if they are coastal, because shipping costs are smaller than the range of PLCOAs across the globe. However, the capacity of these excellent locations may be constrained by land availability, which limits the capacity of individual sites, and the total global ammonia production capacity. Unless land can be secured in good locations, meeting global chemical energy demand will require the use of sites whose delivered ammonia price is substantially higher than the optimal price. Importantly, this conclusion is agnostic to the hydrogen carrier; the impact of land considerations is likely to be similar even if liquid hydrogen, methanol, a liquid organic hydrogen carrier, or synthetic hydrocarbons are used in place of ammonia. Three remedies are possible to mitigate this constraint: the identification of more sites with excellent ammonia production capabilities; obtaining more land in the best locations; or development of affordable renewable technologies which are less land-intensive, such as more space-efficient onshore generation or offshore wind and solar capabilities.

Further research is required on four fronts. Firstly, a more precise estimation of the demand for chemical energy vectors in 2050 is required; the cost of ammonia depends strongly on demand, and it will inform the extent to which additional locations and additional land are required in order to satisfy chemical energy demand. As part of demand estimation, further analysis on the distribution of ammonia as marine fuel will be required. Because the properties of ammonia differ from the heavy fuel oil used today, the frequency of ship refueling will change, and hence, the ports at which bunker fuel is required will also change. Secondly, the model used in this research is based on annual average production; however, the provision of ammonia will vary seasonally as wind and solar patterns vary. This may render sites close to demand centers less suitable for ammonia supply, or sites further away more optimal. It may also create bidirectional trade of ammonia between countries where supply and demand cycles are temporally misaligned. Thirdly, several factors will influence the future cost of ammonia, including technology improvements, economies of mass production, identification of optimal sites, and climate variation which may impact the suitability of the best sites for renewable energy generation. Further research to understand how these various factors will impact the PLCOA at different locations, and the selection of those locations, will refine the ammonia distribution model developed here. Finally, estimates of land availability in this model are not country specific; this may have underestimated availability in countries with low population density (e.g. Australia) and overestimated availability in countries with high population density (e.g. India). Refining renewable energy capacity data would provide a clearer picture of which countries are best placed to produce ammonia for future global markets.

STAR★METHODS

Detailed methods are provided in the online version of this paper and include the following:

- KEY RESOURCES TABLE
- RESOURCE AVAILABILITY

SUPPLEMENTAL INFORMATION

Supplemental information can be found online at https://doi.org/10.1016/j.isci.2021.102903.

ACKNOWLEDGMENTS

The work here was supported financially by the Rhodes Trust. The use of MATLAB and its toolboxes was under an academic license. AIS data was provided by the Oxford School of Geography.

AUTHOR CONTRIBUTIONS

Conceptualization: N.S. & R. B-A., Methodology: N.S., Software: N.S, Validation: R. B-A., Writing – Original Draft: N.S., Writing – Review & Editing: R. B-A., R. N-L., Data Curation, R. N-L.

DECLARATION OF INTERESTS

There are no conflicts to declare.

Received: May 14, 2021
Revised: June 8, 2021
Accepted: July 21, 2021
Published: August 20, 2021

REFERENCES

Al-Breiki, M., and Bicer, Y. (2020). Technical assessment of liquefied natural gas, ammonia and methanol for overseas energy transport based on energy and exergy analyses. Int. J. Hydrogen Energy *45*, 34927–34937.

Armijo, J., and Philibert, C. (2020). Flexible production of green hydrogen and ammonia from variable solar and wind energy: case study of Chile and Argentina. Int. J. Hydrogen Energy *45*, 1541–1558.

Ash, N., and Scarbrough, T. (2019). Sailing on Solar: Could Green Ammonia Decarbonise International Shipping? (Environmental Defense Fund).

Asian Renewable Energy Hub (2020). https://asianrehub.com/about/.

Australian Department of Industry (2020). Exploring Australia's Hydrogen Future with Germany. https://www.minister.industry.gov.au/ministers/taylor/media-releases/exploring-australias-hydrogen-future-germany.

Austria Energy (2021). Green Hydrogen. https://www.austriaenergy.com/en/green-hydrogen/.

Babarit, A., Gilloteaux, J.-C., Clodic, G., Duchet, M., Simoneau, A., and Platzer, M.F. (2018). Techno-economic feasibility of fleets of far offshore hydrogen-producing wind energy converters. Int. J. Hydrogen Energy *43*, 7266–7289.

Ban, J., Arellano, J., Aguilera, R., and Tallett, M. (2015). World Oil Outlook, OPEC. https://www.opec.org/opec_web/static_files_project/media/downloads/publications/WOO%202015.pdf.

Bartels, J. (2008). A Feasibility Study of Implementing an Ammonia Economy, MSc Thesis (Iowa State University).

Bellini, E. (2021). Brazil May Host $5.4bn Green Hydrogen Plant. https://www.pv-magazine.com/2021/03/03/brazil-masy-host-5-4bn-green-hydrogen-plant/.

Cesaro, Z., Ives, M., Nayak-Luke, R., Mason, M., and Bañares-Alcántara, R. (2021). Ammonia to power: Forecasting the levelized cost of electricity from green ammonia in large-scale power plants. Appl. Energy *282*, 116009. https://doi.org/10.1016/j.apenergy.2020.116009.

Couper, J., Penney, W., Fair, J., and Walas, S. (2012). 6 - flow of fluids. In Chemical Process Equipment (Third Edition), Third Edition, J.R. Couper, W.R. Penney, J.R. Fair, and S.M. Walas, eds. (Butterworth-Heinemann), pp. 83–119. https://www.sciencedirect.com/science/article/pii/B9780123969590000069.

CSIRO (2020). Queensland Solar Hydrogen Facility. https://research.csiro.au/hyresource/queensland-solar-hydrogen-facility/#:~:text=Austrom%20Hydrogen%20have%20announced%20plans,Gladstone%20for%20export%20of%20hydrogen.

Economic Research Institute for ASEAN and East Asia (2018). Investment in LNG Supply Chain Infrastructure Estimation, ERIA, Jakarta, book section 6, 67–80. https://globallnghub.com/wp-content/uploads/2018/05/ERIA_RPR_FY2016_7b_Chapter_6.pdf.

Ennassiri, Y., Belhaj, I., and Bouzekri, H. (2019). Techno-Economic assessment of hydrogen production from VRE in Morocco case study: Laayoune, Ouarzazate, Midelt. In 2019 7th International Renewable and Sustainable Energy Conference (IRSEC), pp. 1–6.

Fasihi, M., Weiss, R., Savolainen, J., and Breyer, C. (2021). Global potential of green ammonia based on hybrid pv-wind power plants. Appl. Energy *294*, 116170. https://www.sciencedirect.com/science/article/pii/S0306261920315750.

Fernandez, C.A., and Hatzell, M.C. (2020). 'Editors' Choice–economic considerations for low-temperature electrochemical ammonia production: Achieving haber-bosch parity'. J. Electrochem. Soc. *167*, 143504.

Fúnez Guerra, C., Reyes-Bozo, L., Vyhmeister, E., Jaén Caparrós, M., Salazar, J.L., and Clemente-Jul, C. (2020). Technical-economic analysis for a green ammonia production plant in Chile and its subsequent transport to Japan. Renew. Energy *157*, 404–414.

Food and Agriculture Organisation of the UN (2021). Faostat. http://www.fao.org/faostat/en/#data/RL.

Gerbert, P., Herhold, P., Burchardt, J., Schönberger, S., Rechenmacher, F., Kirchner, A., Kemmler, A., and Wünsch, M. (2018). Klimapfade

für Deutschland. https://image-src.bcg.com/Images/Klimapfade-fuer-Deutschland_tcm108-181356.pdf.

Global Energy Assessment (2012). Global Energy Assessment - toward a Sustainable Future (Cambridge University Press). www.globalenergyassessment.org.

Hank, C., Sternberg, A., Köppel, N., Holst, M., Smolinka, T., Schaadt, A., Hebling, C., and Henning, H.-M. (2020). Energy efficiency and economic assessment of imported energy carriers based on renewable electricity. Sustain. Energy Fuels *4*, 2256–2273.

Hochman, G., Goldman, A.S., Felder, F.A., Mayer, J.M., Miller, A.J.M., Holland, P.L., Goldman, L.A., Manocha, P., Song, Z., and Aleti, S. (2020). Potential economic feasibility of direct electrochemical nitrogen reduction as a route to ammonia. ACS Sustain. Chem. Eng. *8*, 8938–8948. https://doi.org/10.1021/acssuschemeng.0c01206.

Homan, H., and Klass, C. (2020). LNG Freight rates. https://www.argusmedia.com/en/hubs/lng.

International Renewable Energy Agency (2019). Hydrogen: A Renewable Energy Perspective. https://www.irena.org/publications/2019/Sep/Hydrogen-A-renewable-energy-perspective.

Jan, B., Sugungun, M., Benmerabet, M., and Salo, R. (2020). Oil Demand (OPEC), pp. 129–131, book section 3.

Japanese Ministry of Economy, Trade and Industry (2021). Overview of Japan's Green Growth Strategy through Achieving Carbon Neutrality in 2050. https://www.meti.go.jp/english/press/2020/pdf/1225_001a.pdf.

Jones, J. (2020). First Green Hydrogen Projects Emerge in Chile. https://www.powerengineeringint.com/hydrogen/first-green-hydrogen-projects-emerge-in-chile/.

Kakoulaki, G., Kougias, I., Taylor, N., Dolci, F., Moya, J., and Jäger-Waldau, A. (2021). 'Green hydrogen in europe – a regional assessment: substituting existing production with electrolysis powered by renewables'. Energy Convers. Management *228*, 113649.

Keating, C. (2020). Beijing Jingneng Plots 5GW Wind-Solar-Hydrogen-Storage Hub in Inner Mongolia. https://www.pv-tech.org/beijing-jingneng-plans-5gw-solar-wind-hydrogen-storage-complex-in-inner-mon/.

Leighty, W., and Holbrook, J. (2012). Alternatives to electricity for transmission, firming storage, and supply integration for diverse, stranded, renewable energy resources: Gaseous hydrogen and anhydrous ammonia fuels via underground pipelines. In WHEC 2012 Conference Proceedings – 19th World Hydrogen Energy Conference, *29*WHEC 2012 Conference Proceedings – 19th World Hydrogen Energy Conference (JPdL International), pp. 332–346.

Lim, D., Plymill, A., Paik, H., Qian, X., Zecevic, S., Chisholm, C., and Haile, S. (2020). Solid acid electrochemical cell for the production of hydrogen from ammonia. Joule *4*, 2338–2347. https://doi.org/10.1016/j.joule.2020.10.006.

Mayyas, A., Ruth, M., Pivovar, B., Bender, G., and Wipke, K. (2019). Manufacturing Cost Analysis for Proton Exchange Membrane Water Electrolyzers. https://www.nrel.gov/docs/fy19osti/72740.pdf.

Moffatt and Nichol (2005). Evaluation of a Single Point Mooring Offshore the Port of Los Angeles. https://kentico.portoflosangeles.org/getmedia/ce2902bd-c61b-45dd-bef4-c390938c8047/Appendix_F_Single_Point_Mooring_Evaluation.

Moriarty, P., and Honnery, D. (2012). What is the global potential for renewable energy? Renew. Sustain. Energy Rev. *16*, 244–252.

National Institute for Standards and Technology (2020). Chemistry Webbook. https://webbook.nist.gov/chemistry/.

Nayak-Luke, R., and Bañares-Alcántara, R. (2020). Techno-economic viability of islanded green ammonia as a carbon-free energy vector and as a substitute for conventional production. Energy Environ. Sci. *13*, 2957–2966. https://doi.org/10.1039/D0EE01707H.

Nayak-Luke, R., Forbes, C., Cesaro, Z., Banares-Alcantara, R., and Rowenhurst, K. (2020). Techno-economic Aspects of Production, Storage, and Distribution of Ammonia, *8* (Elsevier), pp. 191–209.

Osman, O., Sgouridis, S., and Sleptchenko, A. (2020). Scaling the production of renewable ammonia: a techno-economic optimization applied in regions with high insolation. J. Clean. Prod. *271*, 121627.

Platts, S.G. (2021). Portworld Distance Calculation. https://www.portworld.com/map.

Raaijmakers, R. (2012). Offshore terminals for the transportation of LPG. https://www.porttechnology.org/wp-content/uploads/2019/05/PT26-22.pdf.

Rogers, H. (2018). The LNG shipping forecast: costs rebounding, outlook uncertain. https://www.oxfordenergy.org/wpcms/wp-content/uploads/2018/02/The-LNG-Shipping-Forecast-costs-rebounding-outlook-uncertain-Insight-27.pdf.

Ruiz, P., Nijs, W., Tarvydas, D., Sgobbi, A., Zucker, A., Pilli, R., Jonsson, R., Camia, A., Thiel, C., Hoyer-Klick, C., et al. (2019). ENSPRESO - an open, EU-28 wide, transparent and coherent database of wind, solar and biomass energy potentials. Energy Strategy Rev. *26*, 100379.

Salmon, N., and Bañares-Alcántara, R. (2021). Green ammonia as a spatial energy vector: a review. Sustain. Energy Fuels, 2814–2839. https://doi.org/10.1039/D1SE00345C.

Sanchez, A., and Martín, M. (2018). Optimal renewable production of ammonia from water and air. J. Clean. Prod. *178*, 325–342.

Schmidt, J., Gruber, K., Klingler, M., Klöckl, C., Ramirez Camargo, L., Regner, P., Turkovska, O., Wehrle, S., and Wetterlund, E. (2019). A new perspective on global renewable energy systems: why trade in energy carriers matters. Energy Environ. Sci. *12*, 2022–2029. https://doi.org/10.1039/c9ee00223e.

ShipNext. (2021). Ports. https://shipnext.com/port/.

Songhurst, B. (2014). LNG Plant Cost Escalation. https://www.oxfordenergy.org/wpcms/wp-content/uploads/2014/02/NG-83.pdf.

Taillon, M. (2016). CF Industries Announces Start-Up of New Ammonia Plant at Donaldsonville Nitrogen Complex. https://ascensionedc.com/cf-industries-announces-start-new-ammonia-plant-donaldsonville-nitrogen-complex/#:~:text=Total%20annual%20gross%20ammonia%20capacity.

Tattini, J., and Teter, J. (2020). International Shipping - IEA Tracking Report. https://www.iea.org/reports/international-shipping-resources.

US Energy Information Administration (2017). World Oil Transit Chokepoints. https://www.eia.gov/international/content/analysis/special_topics/World_Oil_Transit_Chokepoints/wotc.pdf.

Valera-Medina, A., Xiao, H., Owen-Jones, M., David, W., and Bowen, P. (2018). Ammonia for power. Prog. Energy Combust. Sci. *69*, 63–102. http://orca.cf.ac.uk/115540/1/180910%20JPECS%20Ammonia.pdf.

Van Hoecke, L., Laffineur, L., Campe, R., Perreault, P., Verbruggen, S.W., and Lenaerts, S. (2021). Challenges in the use of hydrogen for maritime applications. Energy Environ. Sci. *14*, 815–843. https://doi.org/10.1039/D0EE01545H.

Vasquez, A., and Hapes, B. (2019). Europe's Largest Single-Train Ammonia Plant Successfully Started up with KBR Technology. https://www.kbr.com/en/insights-events/press-release/europes-largest-single-train-ammonia-plant-successfully-started-kbr.

Wärtsilä. (2021). Encyclopedia of Marine Technology. https://www.wartsila.com/encyclopedia/term/gas-carrier-types.

Yang, C., and Ogden, J. (2007). Determining the lowest-cost hydrogen delivery mode. Int. J. Hydrogen Energy *32*, 268–286. https://doi.org/10.1016/j.ijhydene.2006.05.009.

Yoo, B., Choi, D., Kim, H., Moon, Y., Na, H., and Lee, S. (2013). Development of CO2 terminal and CO2 carrier for future commercialized CCS market. Int. J. Greenh. Gas Control. *12*, 323–332. https://www.sciencedirect.com/science/article/pii/S175058361200271X.

Zauner, A., Böhm, H., Rosenfeld, D., and Tichler, R. (2019). Innovative Large-Scale Energy Storage Technologies and Power-To-Gas Concepts after Optimization: Analysis on Future Technology Options and on Techno-Economic Optimization. https://www.storeandgo.info/fileadmin/downloads/deliverables_2020/Update/2019-07-04_STOREandGO_D7.7_accepted.pdf.

STAR★METHODS

KEY RESOURCES TABLE

REAGENT or RESOURCE	SOURCE	IDENTIFIER
Software and algorithms		
Shipping distances	S&P Global	Portworld Distance Calculator
Production levelised costs of ammonia	Nayak-Luke and Bañares-Alcántara	https://doi.org/10.1039/d0ee01707h
Port data	ShipNext	https://shipnext.com/port/
Available land areas	Food and Agriculature Organisation of the UN	http://www.fao.org/faostat/en/data/RL
Fluid properties	National Institute of Standards and Technology	https://webbook.nist.gov/chemistry/

RESOURCE AVAILABILITY

Lead contact

Requests for further information should be directed to the lead contact, René Bañares-Alcántara (rene.banares@eng.ox.ac.uk)

Materials availability

This study did not generate new unique physical materials.

Data and code availability

The input data are available in the key resources table and in the body of the text. The authors believe there are enough details within the work to reproduce its results, and the code associated with this article is available from the Lead Contact on reasonable request.

METHOD DETAILS

Model description

The modeling goal is to minimise the delivered levelised cost of ammonia, which is calculated according to (3) in the main text.

The CAPEX and OPEX at each set of nodes are calculated according to:

$$OPEX_{S_{Ex}} = \sum_{Ex \in S_{Ex}, Po \in S_{Po}} PLCOA_{Ex} F_{Ex,Po}$$

$$OPEX_{S_{Ex},S_{Po}} = \sum_{Ex \in S_{Ex}, Po \in S_{Po}} F_{Ex,Po} D_{Ex,Po} C_{StandardPipe}$$

$$CAPEX_{S_{Po}} = \sum_{Po \in S_{Po}} \left(V_{Po} \frac{C_{StandardTank}}{P_{StandardTank}} + x_{Po} C_{NewPort} \right)$$

$$OPEX_{S_{Po}} = \sum_{Po \in S_{Po}} \left(V_{Po} \frac{C_{StandardTank}}{P_{StandardTank}} P_{TankO\&M} + x_{Po} C_{NewPort} P_{TankO\&M} + V_{Po} C_{Boiloff} \right)$$

$$OPEX_{S_{Po,Im}} = \sum_{Po \in S_{Po}, Im \in S_{Im}} F_{Po,Im} C_{Po,Im}$$

Because of the linearisation process, the costs of ammonia production, pipeline transport and ocean transport are treated as operating costs.

The minimisation is subject to the following constraints:

$$Cap_{Ex} \geq \sum_{Po \in S_{Po}} F_{Ex,Po} \quad \forall \; Ex \in S_{Ex}$$

$$Cap_{Im} \leq \sum_{Po \in S_{Po}} F_{Po,Im} \quad \forall\ Im \in S_{Im}$$
$$\sum_{Ex \in S_{Ex}} F_{Ex,Po} = \sum_{Im \in S_{Im}} F_{Po,Im} \quad \forall\ Po \in S_{Po}$$
$$V_{Po} \geq x_{Ex} 1.5 P_{VMax_{Po}} \quad \forall Po \in S_{Po}$$
$$V_{Po} \geq \sum_{Ex} F_{Ex,Po}/52 \quad \forall Po \in S_{Po}$$

Pipelines are only able to deliver ammonia to ports within the same region, which is achieved using the following constraint:

$$F_{Ex,Po} D_{Ex,Po} \geq 0 \quad \forall\ Ex \in S_{Ex} \forall\ Po \in S_{Po}$$

$D_{Ex,Po}$ is set to -1 for pipeline paths between exporters and ports that are not within the same region, which given the above constraint will stop those exporters transporting ammonia to those ports.

If suppliers are active they must produce a minimum of 1 MMTPA of ammonia per year. This is achieved using two constraints:

$$\frac{\sum_{Po \in S_{Po}} F_{Ex,Po}}{\sum_{Ex \in S_{Ex}} Cap_{Ex}} \leq x_{Ex} \quad \forall\ Ex \in S_{Ex}$$
$$x_{Ex} MinSize \leq \sum_{Po \in S_{Po}} F_{Ex,Po} \quad \forall\ Ex \in S_{Ex}$$

The denominator of the first constraint is simply the total supply capacity of all suppliers in the model; it will always be greater than or equal to the flow between any one exporter and port, and therefore is suitable to normalise the value for comparison to a binary integer variable.

The model must also determine if a port is active, or it will enforce minimum storage tank sizes on ports which are not used in the model. The port is switched off if (i) There is no exporter which sends ammonia to that port, or (ii) There are no ships big enough to dock in it. Mathematically:

$$\frac{\sum_{Ex \in S_{Po}} F_{Ex,Po}}{\sum_{Ex \in S_{Ex}} Cap_{Ex}} \leq x_{Po} \quad \forall\ Po \in S_{Po}$$
$$D_{Po,Ex} \geq x_{Po} - 1 \quad \forall\ Po \in S_{Po} \quad \forall\ Ex \in S_{Ex}$$

The second equation prevents the port from being active if the distance from a port to any exporters is -1 or less; the distance parameter is set to -1 if a trip is banned because the ship is too small. If the second constraint above prevents a port from operating, then the first constraint will stop any ammonia from flowing to that port.

This results in a model with 200,47 variables, 224 of which are integers. There are 15,559 rows.

Notation

Decision variables	
Decision variables	
$F_{i,j}$	Flow in t/year of ammonia from node i to node j (defined for both Exporters to ports, and ports to importers)
x_{Ex}	Binary variable indicating if a supplier is active
x_{Po}	Binary variable indicating if a new port has been built; can only be true if the exporter is designated as coastal
V_{Po}	Volume (in m^3) of tank storage required at a nominated port

Calculated variables	
Major variables calculated from decision variables	
$CAPEX_{S_i}$	Total Expected capital cost for a set of nodes S_1 in millions of USD
$CAPEX_{S_i,S_j}$	Total Expected capital cost for ammonia transport from a set of nodes S_i to a set of nodes S_j in millions of USD
$OPEX_{S_i}$	Total Expected operating cost for a set of nodes S_i in millions of USD
$OPEX_{S_i,S_j}$	Total Expected operating cost for ammonia transport from a set of nodes S_i to a set of nodes S_j in millions of USD
NPV_{S_i}	Expected net present value (NPV) for a set of nodes S_i in millions of USD
NPV_{S_i,S_j}	Expected net present value (NPV) for ammonia transport from a set of nodes S_i to a set of nodes S_j in millions of USD

Major parameters	
Major parameters	
S_{Ex}	Set of ammonia production nodes i.e. Exporters
S_{Po}	Set of ammonia port nodes
S_{Im}	Set of ammonia importing countries i.e. Importers
Cap_i	Capacity of a nominated element of a set S_i in tpa (equivalent to supply capacity for exporters and demand for importers)
$D_{i,j}$	estimated distance from node i to node j in km (based on arc length between points). Equal to −1 if transport between nodes is not allowed (e.g. if it would require a pipeline over ocean)
MinCap	Minimum allowable capacity of an ammonia plant to display linear price behavior (Estimated as 1MMTPA in linearization section)
ρ_{NH_3}	Density of liquid ammonia = 604 kg/m^3
$PLCOA_{Ex}$	Production LCOA at a nominated exporter in USD/t

General parameters	
General parameters	
G_{WH}	Annual working hours = 8,424 hr
G_{EY}	Equivalent years of operation; a $1 increase in OPEX will increase the NPV by G_{EY} (calculated in methodology section)
G_I	Discount rate = 0.07
G_y	Project lifetime = 20 years

Cost parameters	
Cost parameters	
C_{Grid}	General power cost = 80 USD/MW
C_{Steel}	Cost per tonne of steel = 5,000 USD/t
$C_{StandardPump}$	Cost of a standard sized ammonia pump = 10,000 USD
$C_{StandardPipe}$	Linearised cost/levelised t/km of ammonia pipeline, including pumping costs
$C_{StandardTank}$	Cost of a standard volume ammonia tank at a port = 28.5 million USD
$C_{Boiloff}$	Cost per storage volume to re-condense boil off = 14 USD/t installed storage/year (see calculation approach in linearization Section)
$C_{Ocean_{Po,Im}}$	Cost per ton of ammonia transport between a port Po and Im. Equal to −1 if a port is too small to allow any ships to berth; otherwise see method in ocean transport costs section

Land transport variables and sets	
Land transport variables and sets	
S_{λ}	Allowable set of pipeline linear densities for standard pipelines
S_D	Allowable set of pipeline diameters for standard pipelines
S_A	Allowable set of pipeline areas for standard pipelines
$L_{\lambda_{Ex,Po}}$	Linear density of single pipeline from an exporter to a port in kg/m, $\in S_{\lambda}$
$L_{D_{Ex,Po}}$	Diameter of single pipeline from an exporter to a port in m, $\in S_D$
$L_{A_{Ex,Po}}$	Area of single pipeline from an exporter to a port in m^2, $\in S_A$
$L_{n_{Ex,Po}}$	Number of pipelines from an exporter to a port
$L_{P_{Ex,Po}}$	Number of pumps on a single pipeline
$v_{Ex,Po}$	Average velocity of ammonia in pipeline from an exporter to a port in m/s
$\dot{W}_{Ex,Po}$	Average power of pump for a single pipeline from an exporter to a port in MW
$f_{Ex,Po}$	Friction factor in pipeline from an exporter to a port

Land transport parameters	
Land transport parameters	
L_C	Conversion factor for ammonia from t/year to m^3/s
L_{DF}	Distance factor for pipeline
L_{HF}	Head loss factor for pipeline

(*Continued on next page*)

Continued	
Land transport parameters	
L_{η}	Pump efficiency
L_{FF}	Fabrication factor
L_{SS}	Standard pump size
L_{SF}	Pump scale factor
L_{OM}	Pipeline O& M fraction

Port parameters and variables	
Port parameters	
$P_{VMax_{Po}}$	Maximum volume of ship allowed in port (in m^3)
$P_{StandardTank}$	Volume of standard ammonia tank (in m^3)
$P_{TankO\&M}$	O&M fraction associated with ammonia tank
$P_{PortO\&M}$	O&M fraction associated with a new port

Pipeline cost estimation

In order to demonstrate the linear pipeline costs at scale, and to estimate a suitable factor for pipeline costs per kilometre, the cost of an ammonia pipeline was rigorously estimated as described below. The results of this estimation are shown in Figure 1C. For that figure, the distance between ammonia producer and port was taken as 100 km; costs are almost a linear function of distance (only pump costs are non-linear, and these represent a small fraction of total costs). A factor of 1.2 was applied to relate the direct distance between locations to the pipeline length to reflect the route deviations which may be required by the pipeline.

The pipeline CAPEX itself was determined by a pipeline cost (P_S) multiplied by an installation factor (P_{FF}) which was calibrated to be equal to the published costs in Nayak-Luke et al. (Nayak-Luke et al., 2020). The pump power was determined based on the head loss in the pipeline, estimated using the friction factor and an additional factor of 1.1 to account for minor losses in the pipe.

The pump CAPEX was scaled from a quotation received for an ammonia pump from a vendor; the pump power was used as the representative unit size, and a scaling factor of 0.7 was applied. Pumps are required for approximately every 128 km of pipeline length (Nayak-Luke et al., 2020). The pipeline OPEX was calculated based on the power consumption, and an O&M fraction of 0.5% of all CAPEX. The equations representing this description are summarised below; the NPV was subsequently calculated methodology section.

The NPV of the pipeline was then optimised at a range of flow-rates from 10^5 to 10^7 tpa, constraining the pipeline to standard pipe sizes as described in Couper and Penney(Couper et al., 2012). If the optimal pipe size exceeded the largest standard pipe size available (30″) then the system runs multiple parallel pipelines. Because the pipeline is constrained to integer diameters, the levelised cost of ammonia transport is not a smooth function of ammonia production rate. Using those results, the cost per levelised ton per km of pipeline ($C_{StandardPipe}$) were estimated using a linear regression between 1 and 10 MMTPA of ammonia. The overall results are in the order of 2 USD/levelised t/km, which are comparable to the estimate in Leighty and Holbrook (Leighty and Holbrook, 2012).

$$v_{Ex,Po} = \frac{F_{Ex,Po} L_C}{L_{A_{Ex,Po}} L_{n_{Ex,Po}}}$$

$$\dot{W}_{Ex,Po} = 10^{-3} \cdot \left[\frac{\rho_{NH_3} F_{Ex,Po} L_C v_{Ex,Po}^2 D_{Ex,Po} f_{Ex,Po}}{2 L_{D_{Ex,Po}} L_{n_{Ex,Po}}} \right] \left[\frac{L_{DF} L_{HF}}{L_{\eta}} \right]$$

$$CAPEX_{Ex,Po} = 10^{-6} L_{n_{Ex,Po}} \cdot \left[L_{\lambda_{Ex,Po}} D_{Ex,Po} L_{DF} C_{Steel} L_{FF} + L_{P_{Ex,Po}} C_{Standard\ \ Pump} \left(\frac{\dot{W}_{Ex,Po}}{L_{SS} L_{P_{Ex,Po}}} \right)^{L_{SF}} \right]$$

$$OPEX_{Ex,Po} = 10^{-6} \left[L_{n_{Ex,Po}} \dot{W}_{Ex,Po} C_{Grid} G_{WH} \right] + L_{OM} CAPEX_{Ex,Po}$$